Robust trajectory-tracking for nonholonomic wheel mobile robots using a PSO-tuned control approach

Ngoc Trung Dang[1*]

[1]*Thai Nguyen University of Technology*
[*]*Corresponding author E-mail: trungcsktd@tnut.edu.vn*
DOI: https://doi.org/10.64032/mca.v29i3.339

Abstract

This paper addresses the trajectory-tracking problem for nonholonomic wheeled mobile robots subjected to model uncertainties and unknown external disturbances. In contrast to existing approaches that concentrate primarily on the kinematic control loop, this paper adopts a hierarchical control structure for the wheel mobile robot, including an outer kinematic loop and an inner dynamic loop. For the dynamic control loop, a dynamic controller combining integral terminal sliding mode control and a disturbance observer is developed to achieve disturbance rejection and chattering reduction. For the kinematic control loop, the kinematic controller is designed for accurate trajectory tracking control. Based on the Lyapunov stability theory, the stability analysis is given for both the disturbance observer and the double-loop tracking controller. Furthermore, the Particle Swarm Optimization algorithm is employed to optimize the control gains, thereby enhancing the overall performance of the control system. The simulation result using MATLAB software is conducted to confirm the effectiveness of the proposed method.

Keywords: *Nonholonomic wheel mobile robot, Trajectory-tracking control, Disturbance observer, Particle swarm optimization*

1. Introduction

Due to the advantages of high flexibility, easy operation, fast and stable motion, high energy efficiency, and strong system integration, wheeled mobile robots (WMRs) have been widely used in various fields, such as autonomous navigation, surveillance, smart warehousing, industrial inspection, environmental monitoring, autonomous delivery services, medical care, and so on [1, 2, 3, 4, 5].

In general, the problem of trajectory-tracking control for the WMRs has remained a core issue and has consistently attracted considerable attention in the fields of robotics and industrial control. It is well known that designing control systems for the WMRs must address inherent challenges such as nonlinear coupling, nonholonomic constraints, and underactuated dynamics [12]. Furthermore, it is noteworthy that WMRs are often required to carry additional payloads such as manipulators, sensors, or auxiliary batteries [13]. These additions result in variations in payload mass and its spatial distribution, which constitute a major source of parameter uncertainties in mobile robots, particularly influencing the system's mass and moment of inertia. Besides, to enhance the applicability of the system in real-world tasks, external disturbances should be taken into account to improve the robot's performance. In recent years, various control approaches have been attempted to tackle these control issues of the WMR, including PID control [6], Sliding mode control (SMC) [7, 8], Fuzzy control [9], Neural network-based control [11], Model predictive control (MPC) [10] etc. Although these control approaches achieve some outstanding performance for the WMRs, such as fast error convergence, robustness against uncertainties and external disturbances, they also have some drawbacks. For instance, the chattering effect is often neglected, the issues of optimality and controller parameter selection are not thoroughly addressed, and the computational burden remains significant.

In the existing research results, Sliding Mode Control (SMC) is well established in the literature as an effective nonlinear control methodology. Its extensive application within the field of control engineering systems is primarily due to its intrinsic robustness to disturbances and model uncertainties. The SMC technique has been widely employed for trajectory tracking control of the WMRs. For instance, the conventional SMC method is proposed to design the trajectory-tracking controller of the WMRs, ensuring that the tracking errors asymptotically converge to zero. [14]. The recursive terminal SMC [15], fast nonsingular terminal SMC [16], and nonsingular recursive-structure terminal SMC [17] were applied to NWMR to achieve the finite-time tracking error convergence. The core idea of SMC lies in two fundamental problems: constructing the sliding surface and formulating a control law that ensures system stability, typically established via Lyapunov-based analysis [18]. The control input in SMC is generally decomposed into two distinct components: the equivalent control law and the switching control law [19]. The equivalent term is responsible for driving the system trajectory toward the sliding surface, while the switching term maintains the trajectory on the surface and guides it toward the origin. Although the robustness of the SMC technique against model uncertainties and external disturbances can be enhanced by incorporating a robust term with a sufficiently large control gain, typically exceeding the estimated upper bound of disturbances. In particular, if the control gain is set too high, it can cause high-frequency oscillations, usually known as "chattering", which negatively affect control performance and

Received: 13 May 2025; Revised: 31 May 2025; Accepted: 06 June 2025.

may shorten the lifespan of actuators. On the other hand, if the gain is too small, especially when sudden or strong disturbances occur, the control system may not respond effectively, leading to poor tracking accuracy and potential instability. These challenges have motivated the development of advanced robust control strategies that aim to balance disturbance rejection capabilities with smooth control effort.

To overcome this limitation of the SMC technique, the disturbance estimation methods are usually employed to estimate and compensate for these unknown disturbances. The key advantage of the approach is that it only requires the control gain to be slightly larger than the observation error, rather than the disturbance itself, thus significantly mitigating the chattering effect. Based on the highlighted advantages identified in the above analysis, a variety of disturbance rejection techniques have been extensively studied for the WMRs, including Active disturbance rejection control (ADRC) [20], Extended state observer (ESO) [21], and Disturbance observer (DO) [22]. Widely acknowledged for its effectiveness in disturbance estimation techniques, the disturbance observer has been employed in the WMR systems [23, 24] to estimate lumped disturbances, including the model uncertainties and external disturbances. Under the assumption of bounded disturbances and slowly varying noise, the disturbance estimation error will converge to a bounded neighborhood of zero, thereby enabling effective disturbance rejection via a feedforward compensation mechanism.

This paper presents a robust trajectory-tracking control design for a nonholonomic WMR subjected to unknown external disturbances and parameter uncertainties, considering the "chattering" reduction and the optimal control gains. The main contributions of this study are listed as follows

- This study adopts a hierarchical control structure, including a kinematic control loop and a dynamic control loop. It is worth noting that previous studies in [25, 26] only considered the control of the kinematic loop of the nonholonomic WMR, neglecting the dynamic characteristics and interactions between actuators and the robot body, which can lead to degraded performance in practical implementations.
- To achieve the disturbance rejection and the "chattering" reduction, this paper utilizes a nonlinear disturbance observer to estimate and compensate for the lumped disturbances, including unknown external disturbances and model uncertainties. As a result, the WMR is able to achieve accurate trajectory tracking while simultaneously mitigating the chattering effect observed in SMC approaches.
- This paper considers the optimal control gains for both kinematic and dynamic controller by employing Particle Swarm Optimization (PSO) algorithm.

This paper is organized as follows: In **Section 2**, the kinematic and dynamic models of the nonholonomic WMR are established. In **Section 3**, the detail control design of the double-loop control structure based on a disturbance observer and a PSO algorithm are presented. In **Section 4**, a simulation result is provided. Finally, **Section 5** concludes this paper.

2. Wheel mobile robot

2.1 Dynamic model

Consider a nonholonomic wheel mobile robot (WMR) system as illustrated in Fig. 1 and Table. 1. Each of the two drive wheels is equipped with an independent DC motor that generates torque to determine the motion and orientation of the robot.

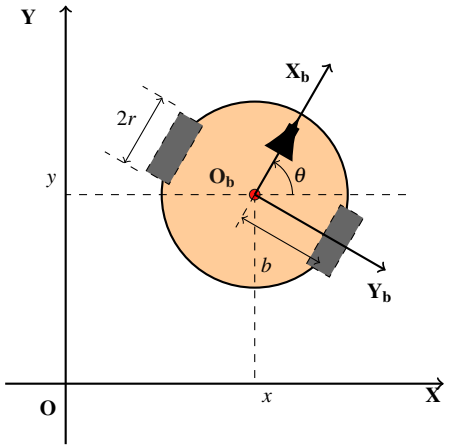

Figure 1: The nonholonomic wheel mobile robot platform

Table 1: Nomination

Symbols	Description	Value	Unit
m_0	the mass of robot	4.5	kg
I_0	the inertia of robot	2.7	m
b	the distance from mass center to each wheel	0.1	m
r	the wheel radius	0.05	kg.m^2
x	the x-axis position		m
y	the y-axis position		m
θ	the yaw angle direction		rad
v	the linear velocity		m/s
w	the angular velocity		rad/s

Define $q = [x, y, \theta]^T \in \mathbb{R}^3$ as the position and orientation of the WMR and $\eta = [v, w]^T \in \mathbb{R}^2$ as linear and angular velocities of the WMR. According to [27], the kinematic model of the nonholonomic WMR is described as follows

$$\dot{q} = \begin{bmatrix} \dot{x} \\ \dot{y} \\ \dot{\theta} \end{bmatrix} = \begin{bmatrix} \cos\theta & 0 \\ \sin\theta & 0 \\ 0 & 1 \end{bmatrix} \begin{bmatrix} u \\ w \end{bmatrix} = S(q)\eta \tag{1}$$

Similar to [31, 33], based on the Euler-Lagrange formulation, the dynamic model of the nonholonomic WMR is described as follows

$$M(q)\ddot{q} + G(q) + F(\dot{q}) + \tau_d = B(q)\tau - A^T(q)\lambda \tag{2}$$

where $\lambda = -m\big(y\sin(\theta) + \dot{x}\cos(\theta)\big)\dot{\theta}$ is the vector of Lagrange multipliers corresponding to the constraint forces, $\tau_d \in \mathbb{R}^3$ is the external disturbance, $\tau = [\tau_l, \tau_r]^T \in \mathbb{R}^2$ are the control torques generated by the left and right driven wheels, respectively. $M(q)$ represents the inertia matrix, $G(q)$ represents gravitational force vector, $F(\dot{q})$ is friction force vector, $B(q)$ represents the control matrix and $A(q)$ represents

constraint Jacobian matrix. The expressions of $M(q)$, $G(q)$, $F(\dot{q})$, $B(q)$, and $A(q)$ are described as follows

$$M(q) = \begin{bmatrix} m & 0 & 0 \\ 0 & m & 0 \\ 0 & 0 & I \end{bmatrix}; \quad B(q) = \frac{1}{r}\begin{bmatrix} \cos\theta & \cos\theta \\ \sin\theta & \sin\theta \\ b & -b \end{bmatrix}$$

$$A^T(q) = \begin{bmatrix} -\sin\theta \\ \cos\theta \\ 0 \end{bmatrix}; \quad G(q) = F(\dot{q}) = \begin{bmatrix} 0 \\ 0 \\ 0 \end{bmatrix}$$

Taking the time derivative of (1), we have

$$\ddot{q} = \dot{S}(q)\eta + S(q)\dot{\eta} \tag{3}$$

Substituting (3) to (2), it yields

$$M(q)\left(\dot{S}(q)\eta + S(q)\dot{\eta}\right) + \tau_d = B(q)\tau - A^T(q)\lambda \tag{4}$$

By multiplying both sides of (4) with $S^T(q)$, the nonholonomic constraint $A^T(q)\lambda$ can be eliminated due to $S^T(q)A^T(q) = 0$, as stated in [32]. Besides, we also obviously have $S(q)M(q)\dot{S}(q) = 0$. The dynamic model of the nonholonomic WMR can be written as follows

$$\bar{M}\dot{\eta} + \bar{\tau}_d = \bar{B}\tau \tag{5}$$

where $\bar{\tau}_d = S^T(q)\tau_d \in \mathbb{R}^2$ and

$$\bar{M} = \begin{bmatrix} m & 0 \\ 0 & I \end{bmatrix}, \qquad \bar{B} = \frac{1}{r}\begin{bmatrix} 1 & 1 \\ b & -b \end{bmatrix}.$$

Assumption 1. *The parameter uncertainties of the WMR are assumed to satisfy the following conditions*

$$\begin{aligned} m &= m_0 + \Delta m \\ I &= I_0 + \Delta I \end{aligned} \tag{6}$$

where $(.)_0$ *and* $\Delta(.)$ *represent the nominal parameters and uncertaties, respectively.*

Hence, the M can be decomposed as follows

$$\bar{M} = \bar{M}_0 + \Delta\bar{M} = \begin{bmatrix} m_0 & 0 \\ 0 & I_0 \end{bmatrix} + \begin{bmatrix} \Delta m & 0 \\ 0 & \Delta I \end{bmatrix} \tag{7}$$

Substituting into (5), it yields

$$\bar{M}_0\dot{\eta} = \bar{B}\tau - (\Delta\bar{M}\dot{\eta} + \bar{\tau}_d) \tag{8}$$

Remark 1. *It is widely known that wheeled mobile robots usually move on a flat surface; therefore, their potential energy can be considered negligible. In addition, the nonholonomic constraints add more limits, restricting the robot's movement to directions at right angles to the axes of the driving wheels. As a result, the robot moves by rolling without slipping*

Remark 2. *Due to the inherent complexity of the dynamic model of the nonholonomic WMR, the kinematic model is commonly utilized in the design of motion controllers to reduce the workload associated with model analysis and control design. However, the dynamic model remains crucial in control design, especially for applications that demand high speeds or carry heavy payloads.*

2.2 Control problem

Consider the desired motion and orientation of the WMR $q_d = [x_d, y_d, \theta_d]^T \in \mathbb{R}^3$ as follows

$$\dot{q}_d = \begin{bmatrix} \dot{x}_d \\ \dot{y}_d \\ \dot{\theta}_d \end{bmatrix} = \begin{bmatrix} \cos\theta_d & 0 \\ \sin\theta_d & 0 \\ 0 & 1 \end{bmatrix} \begin{bmatrix} v_d \\ w_d \end{bmatrix} \tag{9}$$

where $\eta_d = [v_d, w_d]^T \in \mathbb{R}^2$ are the desired linear and angular velocities that can be calculated by

$$\begin{aligned} v_d &= \sqrt{\dot{x}_d^2 + \dot{y}_d^2} \\ w_d &= \dot{\theta}_d = \frac{\dot{x}_d\ddot{y}_d - \ddot{x}_d\dot{y}_d}{\dot{x}_d^2 + \dot{y}_d^2} \end{aligned} \tag{10}$$

Inspired by [29, 30], by carrying out the coordinate transformation from the global frame to the robot frame, the tracking error of the WMR $e_q = [e_x, e_y, e_\theta]^T \in \mathbb{R}^3$ is formulated as follows

$$e_q = \begin{bmatrix} e_x \\ e_y \\ e_\theta \end{bmatrix} = \begin{bmatrix} \cos\theta & \sin\theta & 0 \\ -\sin\theta & \cos\theta & 0 \\ 0 & 0 & 1 \end{bmatrix} \begin{bmatrix} x_d - x \\ y_d - y \\ \theta_d - \theta \end{bmatrix} \tag{11}$$

Thus, the tracking error dynamics of the WMR is formulated as follows

$$\dot{e}_q = \begin{bmatrix} \dot{e}_x \\ \dot{e}_y \\ \dot{e}_\theta \end{bmatrix} = \begin{bmatrix} e_y w + v_d\cos e_\theta - v \\ -e_x w + v_d \sin e_\theta \\ w_d - w \end{bmatrix} \tag{12}$$

The control objective of the mobile robot is to determine the virtual linear and angular velocities and to design control torques that ensure the asymptotic convergence of position and orientation errors to zero. This enables the mobile robot to accurately track a desired reference trajectory.

3. PSO-based robust controller

To tackle this control problem, a hierarchical control structure is proposed, consisting of a kinematic controller and a dynamic controller. The kinematic controller is responsible for generating the desired linear and angular velocity signals based on the reference trajectory and the current tracking errors. The dynamic controller is then designed to ensure that the actual motion of the robot accurately follows the desired velocities while maintaining robustness against model uncertainties and unknown external disturbances.

3.1 Kinematic control loop

For the tracking error dynamics in (12), the virtual linear and angular velocities are adopted as follows

$$\eta_c = \begin{bmatrix} v_c \\ w_c \end{bmatrix} = \begin{bmatrix} c_1 e_x + v_d\cos(e_\theta) \\ w_d + c_2 v_d e_y + c_3 v_d \sin(e_\theta) \end{bmatrix} \tag{13}$$

where c_1, c_2 and c_3 are positive constants to be tuned.

Theorem 1. *For the kinematic model of the nonholonomic WMR (1), based on the tracking error dynamics (12), in the term of the virtual velocities (13), the tracking error* e_q *converges asymptotically to zero as* $t \to \infty$.

Proof. Choosing the Lyapunov candidate function as follows

$$L_1 = \frac{1}{2}e_x^2 + \frac{1}{2}e_y^2 + \frac{1}{c_2}\big(1-\cos(e_\theta)\big) \tag{14}$$

Taking the time derivative of (14) along the tracking error trajectory (12) using (13), it yields

$$\begin{aligned}\dot{L}_1 =& e_x\dot{e}_x + e_y\dot{e}_y + \frac{1}{c_2}\sin(e_\theta)\dot{e}_\theta \\ =& e_x(e_y w + v_d\cos e_\theta - v) + e_y(-e_x w + v_d \sin e_\theta) \\ &+ \frac{1}{c_2}\sin(e_\theta)(w_d - w) \\ =& -c_1 e_x^2 - \frac{c_3}{c_2}v_d\sin^2(e_\theta)\end{aligned} \tag{15}$$

It is noted that the desired linear velocity v_d is positive, thus $L_1 \leq 0$. Based on the Lyapunov stability, the tracking error dynamics (12) is asymptotically stable.

Then, the next work is to design the control torque inputs τ such that the actual velocities $\eta(t)$ asymptotically track the virtual velocities $\eta_c(t)$ as $t \to \infty$. Once the conditions of $\lim_{t\to\infty}|q - q_d| \to 0$ and $\lim_{t\to\infty}|\eta - \eta_d| \to 0$ are met, the WMR achieves trajectory-tracking following the desired reference trajectory.

3.2 Dynamic control loop

The dynamic model of the nonholonomic WMR (8) can be rewritten as

$$\dot{\eta} = H\tau + \varsigma(t) \tag{16}$$

where $H = [\bar{M}_0]^{-1}\bar{B}$ and $\varsigma(t) = [\varsigma_1, \varsigma_2]^T = -[\bar{M}_0]^{-1}(\Delta\bar{M}\dot{\eta} + \bar{\tau}_d) \in \mathbb{R}^2$.

Assumption 2. *It is considered that $\varsigma(t)$ acts as a lumped disturbance, which is an unknown and time-varying vector including external disturbances and uncertain factors. The disturbance and its derivative are assumed to be bounded by $||\varsigma|| \leq \chi_1$ and $||\dot{\varsigma}|| \leq \chi_2$, where χ_1 and χ_2 are positive constants.*

The main approach is based on reconstructing the original system's model (16) to establish a lumped disturbance vector $\varsigma(t)$, which includes model uncertainties and unknown external disturbances. Subsequently, a disturbance observer (DO) is developed to accurately estimate and compensate for the lumped disturbances, while an integral terminal sliding mode control law is designed to achieve accurate trajectory tracking. The stability of the closed-loop system is proven by employing the Lyapunov stability theory.

The following DO is designed as follows

$$\begin{aligned}\dot{z}(t) =& -D(\eta)\big[H\tau + \psi(\eta) + z(t)\big] \\ \hat{\varsigma}(t) =& z(t) + \psi(\eta)\end{aligned} \tag{17}$$

where $\hat{\varsigma}(t) = [\hat{\varsigma}_1, \hat{\varsigma}_2]^T \in \mathbb{R}^2$ is the estimated value of $\varsigma(t)$, $\psi(\eta) \in \mathbb{R}^2$ is a nonlinear function and $D(\eta) = \partial\psi(\eta)/\partial\eta \in \mathbb{R}^{2\times 2}$ is a observer gain. For the dynamic model of the WMR (16), the dynamics of the estimation error $\varsigma_e(t) = \varsigma(t) - \hat{\varsigma}(t)$ can be described as

$$\dot{\varsigma}_e(t) = \dot{\varsigma}(t) - D(\eta)\varsigma_e(t) \tag{18}$$

Theorem 2. *Under the **Assumption 2**, by choosing observer gain $D(\eta)$ that satisfies $D(\eta) - 0.5I_2 \geq 0$, the estimation error dynamics (18) is locally input-to-state stable (ISS). The estimation error is bounded as $t \to \infty$ as $\lim_{t\to\infty}||\varsigma_e(t)|| \leq \sigma$, where σ is a positive constant*

Proof. Choosing the Lyapunov candidate function as

$$L_2 = \frac{1}{2}\varsigma_e^T\varsigma_e \tag{19}$$

Taking the time derivative of (19) along the trajectory of the estimation error dynamics (18), it yields

$$\begin{aligned}\dot{L}_2 =& \varsigma_e^T\dot{\varsigma}_e = \varsigma_e^T\Big(\dot{\varsigma} - D(\eta)\varsigma_e\Big) \\ \leq& -\left(D(\eta) - \frac{1}{2}I_2\right)\varsigma_e^T\varsigma_e + \frac{1}{2}\dot{\varsigma}^T\dot{\varsigma} \\ \leq& -\left(D(\eta) - \frac{1}{2}I_2\right)\varsigma_e^T\varsigma_e + c\end{aligned} \tag{20}$$

where $c = 0.5||\chi_2||^2$ is a positive constant. By choosing $D(\eta) - 0.5I_2 \geq 0$, the estimation error dynamics (18) is locally input-to-state stable.

It is noted that the control torque input is expressed in the following form $\tau = -H^{-1}\hat{\varsigma} + u$. The auxiliary control input $u \in \mathbb{R}^2$ is designed to ensure the velocity tracking error $e_\eta = [e_v, e_w]^T = \eta - \eta_c$ asymptotically converge to zero. The closed-loop error dynamics for e_η can be obtained as

$$\begin{aligned}\dot{e}_\eta =& H\big(-H^{-1}\hat{\varsigma} + u\big) + \varsigma - \dot{\eta}_c \\ =& Hu - \dot{\eta}_c + \varsigma_e\end{aligned} \tag{21}$$

Remark 3. *It is worth emphasizing that the bounded disturbance estimation error ς_e is significantly smaller than its disturbance ς. In robust control strategies, high control gains often lead to undesirable "chattering" problems. The outstanding preponderance is that it only requires significantly smaller control gain, thereby considerably mitigating the "chattering" issue.*

The next work is to design the control input u that achieves the asymptotic stability of the velocity tracking error dynamics (21), considering the influence of the bounded uncertain term ς_e. A integral terminal sliding mode surface is defined as

$$s = e_\eta(t) - e_\eta(0) + \beta\int_o^t \mathrm{sig}^\alpha(e_\eta)d\tau \tag{22}$$

where $0 < \alpha < 1$, $\beta > 0$, and $\mathrm{sig}^\alpha(e_\eta) = |e_\eta|^\alpha\mathrm{sign}(e_\eta)$. Taking the time derivative of s using (21), it yields

$$\dot{s} = Hu - \dot{\eta}_c + \varsigma_e + \beta\mathrm{sig}^\alpha(e_\eta) \tag{23}$$

The control input u can be derived as

$$u = -H^{-1}\big(-\dot{\eta}_c + \beta\mathrm{sig}^\alpha(e_\eta) + k_1 s + k_2\mathrm{sign}(s)\big) \tag{24}$$

where k_1 and k_2 are positive constants to be tuned.

Theorem 3. *For the error dynamic model of the nonholonomic WMR (21), in term of the control input (24), the velocity tracking error e_η is asymptotically stable.*

Proof. Choosing the Lyapunov candidate function as

$$L_3 = \frac{1}{2}s^T s \tag{25}$$

Taking the time derivative of L_3 along the state trajectory of (21) using (24) as

$$\begin{aligned}\dot{L}_3 =& s^T \dot{s} = s^T \left(Hu - \dot{\eta}_c + \varsigma_e + \beta \mathrm{sig}^{\alpha}(e_\eta)\right) \\ =& s_\eta^T \Big(H\big(-H^{-1}\big(-\dot{\eta}_c + \beta \mathrm{sig}^{\alpha}(e_\eta) + k_1 s + k_2 \mathrm{sign}(s)\big)\big) \\ & - \dot{\eta}_c + \varsigma_e + \beta \mathrm{sig}^{\alpha}(e_\eta)\Big) \\ =& -k_1 s^T s - (k_2 \mathrm{sign}(s) - \varsigma_e)\end{aligned} \tag{26}$$

By choosing $k_2 \geq \sigma$, based on the Lyapunov stability, the velocity tracking error dynamics is asymptotically stable. The velocity tracking error will converge to zero as $t \to \infty$.

Remark 4. *In practical application, the discontinuous-time switching term $k_2 sign(s)$ could cause the "chattering" issues. One of the popular techniques that overcomes this limitation is to replace the switching term by smoothing the switching term, usually $sat(s)$. The following $sat(.)$ function can be described as*

$$sat(s) = \begin{cases} \frac{s}{\delta}, & if\ |s| \leq \delta \\ sign(s), & if\ |s| > \delta \end{cases} \tag{27}$$

where $\delta > 0$ is a small constant.

Once, the control input u can be modified as

$$u = -H^{-1}\big(-\dot{\eta}_c + \beta \mathrm{sig}^{\alpha}(e_\eta) + k_1 s + k_2 \mathrm{sat}(s)\big) \tag{28}$$

The control input is designed to guarantee the stability of the position and velocity tracking error dynamics based on the Lyapunov stability theory. The other issue is how to tune the optimized control gains to enhance the performance of the mobile robot without violating stability. For example, in the "chattering" reduction application, it is clear that the control gain k_2 has to be chosen small enough. The problem of tuning the optimal control gains will be discussed in the next section.

3.3 Particle Swarm Optimization

Particle Swarm Optimization (PSO) is a widely used technique for tuning controller parameters due to its effectiveness and simplicity. The core concept involves modeling a group of particles as a population of candidate solutions that explore the search space by following a set of straightforward mathematical rules. Each particle updates its trajectory by considering both its own historically best position and the best position identified by the entire swarm. As more optimal solutions are found, these best positions are iteratively refined, leading the swarm toward convergence on an optimal or near-optimal solution. In contrast to backpropagation-based neural network algorithms [28], PSO typically requires fewer hyperparameters, achieves faster convergence, and maintains a more streamlined algorithmic structure.

The PSO procedure begins by initializing a population of N particles, where each particle encodes a possible solution within a D-dimensional space. Their initial positions X_i and velocities V_i are randomly generated and defined as follows:

$$\begin{aligned}X_i =& l_b + (u_b - l_b) \times \mathrm{rand}(1, D) \\ V_i =& 0\end{aligned} \tag{29}$$

where l_b and u_b are the lower and upper bounds of the control gains, respectively, each particle evaluates the objective function value f at its current position. This value is then compared with the particle's personal best position (P_{best}) and the global best position (G_{best}) found by the swarm. Based on this comparison, each particle updates its velocity and position as follows

$$\begin{aligned}V_i(t+1) =& wV_i(t) + b_1 r_1 \big(P_{best,i} - X_i(t)\big) + b_2 r_2 \big(G_{best,i} - X_i(t)\big) \\ X_i(t+1) =& X_i(t) + \lambda V_i(t+1)\end{aligned} \tag{30}$$

where $i = 1, ..., N$, $b_1, b_2 > 0$ are the learning factors, w is inertia factor, r_1, r_2 are random numbers belong to $[0, 1]$, and $\lambda > 0$ is a scale factor.

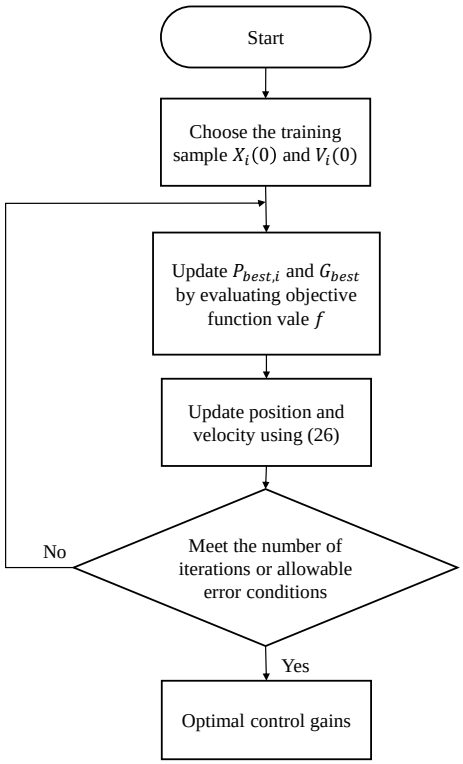

Figure 2: The PSO algorithm

During each iteration, the objective function f is evaluated at the updated position of every particle. If the resulting value surpasses the particle's previous personal best $P_{best,i}$, this personal best is updated accordingly. Likewise, if any particle achieves a better objective value than the current global best $G_{best,i}$, the global best is also updated. This iterative process continues either until a predefined number of iterations is completed or until no further improvement in G_{best} is observed over a specified number of consecutive iterations. Ultimately, the algorithm outputs the optimal value of the objective function and the associated position in the search space, which corresponds to the optimal control gains.

4. Simulation result

In this section, a simulation result conducted using MATLAB software is provided to confirm the effectiveness of the proposed method.

The initial condition of the WMR is set as $q(0) = [1,1,\pi/6]^T$, and the initial position and orientation references are set as $q_d(0) = [1,2,\pi/3]^T$. The desired linear and angular velocities of the WMR are set as $v_d = 2\ (m/s)$ and $w_r = 1\ (rad/s)$, respectively. The parameter uncertainties are assumed as $\Delta m = 0.1m_0$ and $\Delta I = 0.1I_0$. The external disturbance is assumed as follows

$$\tau_d = 0.3 \times \begin{bmatrix} \sin(t+0.5)\sin(0.2t) \\ \cos(t+0.4)\sin(0.2t) \\ \sin(t+0.5)\sin(0.15t) \end{bmatrix} \quad (Nm) \tag{31}$$

The parameter of the disturbance observer and sliding surface (22) is chosen as $D(\eta) = \text{diag}([10,10])$, $\alpha = 0.5$, and $\beta = 2.0$. The PSO algorithm designed for the WMR to find the optimal control gains is set up as:

- Control gain to be optimized: c_1, c_2, c_3, k_1 and k_2
- Objective function:

$$f = \int_0^\infty ||e_q(t)||dt + \int_0^\infty ||e_\eta(t)||dt$$

- Population size: 10 particles
- Maximum number of iterations: 30 iterations
- Lower and upper bounds (l_b, u_b): Parameters are initialized within the range $[0.01, 10]$
- Learning factors (b_1, b_2): 2
- Slace factor (λ): 1
- Inertia factor (w): 0.7

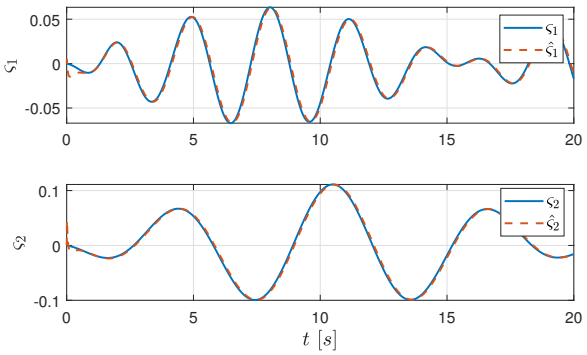

Figure 3: The disturbance estimation

The disturbance estimations of the lumped disturbances $\varsigma(t)$ are shown in Fig. 3. As shown in the Fig. 3, the disturbance observer estimates the lumped disturbances accurately. The Fig. 4 shows both the global best fitness and mean current fitness across iterations, indicating the convergence of the PSO algorithm. The convergence curves clearly show a decreasing trend and stabilize after several iterations. The Fig. 5 presents a comparative simulation between the proposed controller and a conventional ITSMC controller without a nonlinear disturbance observer. The tracking errors of the mobile robot $e_x(t)$, $e_y(t)$, $e_\theta(t)$, $e_v(t)$, and $e_w(t)$ shown for both cases. The results demonstrate that with the proposed controller, all tracking errors converge to zero after approximately 5 seconds, indicating high accuracy and robustness under

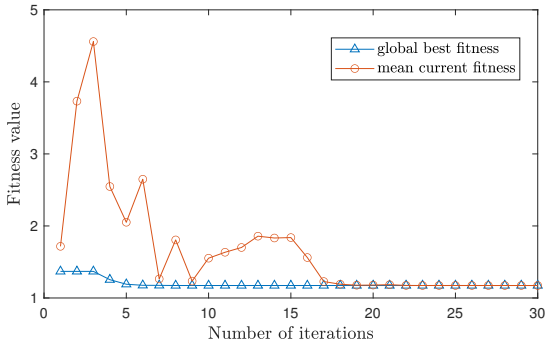

Figure 4: The evolution of the best value found by PSO and the mean current fitness over all particles

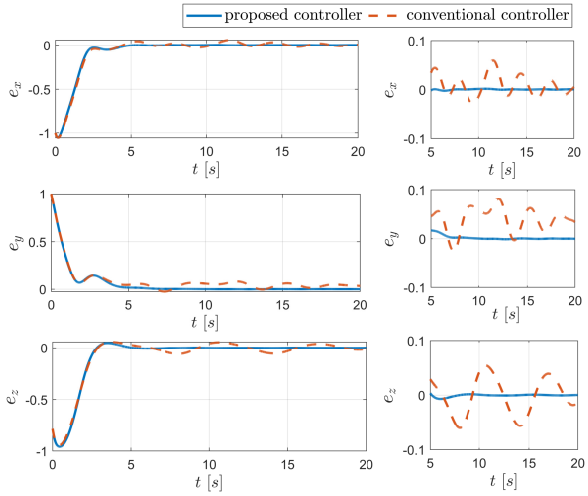

(a) The position and the orientation tracking errors

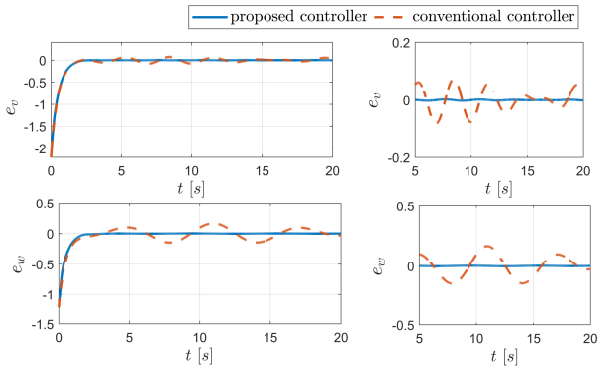

(b) The velocity tracking errors

Figure 5: The tracking errors of the mobile robot

external disturbances. In contrast, the conventional controller fails to cope with the disturbances, while the proposed method achieves better tracking. The position and orientation responses of the mobile robot are shown in Fig. 6. To further demonstrate the trajectory-tracking capability of the mobile robot under the proposed control law, Fig. 7 illustrates the robot's trajectory in three-dimensional space. It is easy to observe that the wheel mobile robot perfectly tracks the desired reference. Furthermore, it is also worth emphasizing that the chattering has been eliminated or significantly reduced by employing a tanh(.) function instead of a switching function and by using Particle Swarm Optimization (PSO) to optimize the control gains.

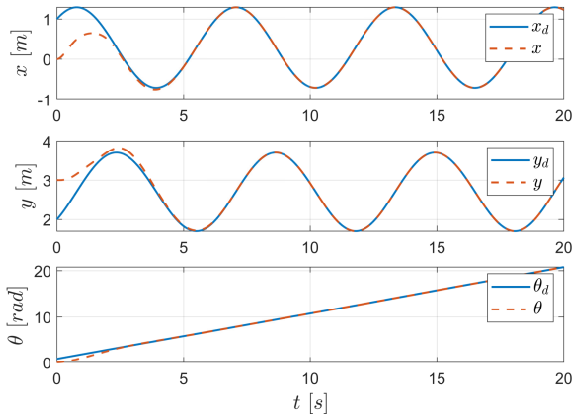

Figure 6: The position and orientation responses of the mobile robot

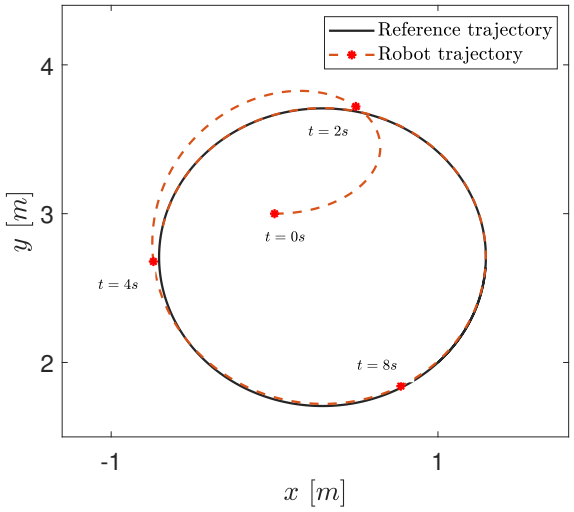

Figure 7: The 2D trajectory of the mobile robot

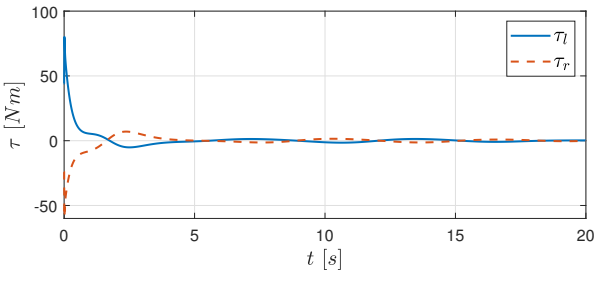

(a) The control torques of the proposed method

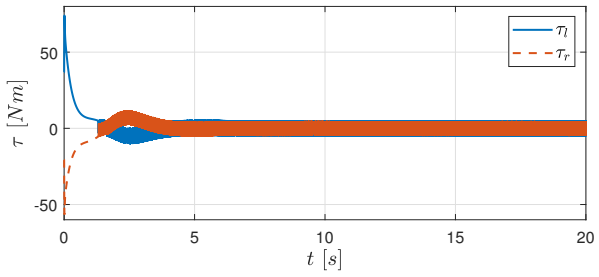

(b) The control torques of the nominal method

Figure 8: The control torques: 8a. proposed controller 8b norminal controller using only terms (12) & (24)

To verify the effectiveness of the proposed method on chattering reduction, a comparison of the control torques generated by the proposed controller and the nominal controller is adopted, as shown in Fig. 8. As shown in Fig. 8b, the control torque with the nominal controller using only terms (12) & (24) is high chattering. On the other hand, the control torque generated by the proposed controller is smooth Fig. 8a, with no abrupt changes observed in the control signals, indicating improved continuity and system stability. This helps to minimize stress on the actuators and the mechanical components of the system.

5. Conclusion

In this paper, a robust trajectory-tracking controller based on the PSO algorithm is developed for the wheel mobile robot system to achieve accurate trajectory tracking performance and strong robustness against lumped disturbances, including unknown external disturbances and parameter uncertainties. The stability analysis for the disturbance observer and the double-loop loop tracking controller has been shown by Lyapunov methods. Furthermore, the "chattering" problem is effectively mitigated by employing the disturbance observer and PSO algorithm. Finally, the robustness and effectiveness of the proposed controller are illustrated by the simulation results.

Acknowledgement

This research was supported by the Research Foundation, which was funded by the Thai Nguyen University of Technology.

References

[1] Ding, Liang, et al. "Definition and application of variable resistance coefficient for wheeled mobile robots on deformable terrain." IEEE Transactions on Robotics 36.3 (2020): 894-909.
[2] Zhao, Lanfei, et al. "The Analysis of trajectory control of non-holonomic mobile robots based on internet of things target image enhancement technology and backpropagation neural network." Frontiers in Neurorobotics 15 (2021): 634340.
[3] Zhao, Ling, et al. "Double-loop tracking control for a wheeled mobile robot with unmodeled dynamics along right angle roads." ISA transactions 136 (2023): 525-534.
[4] Lu, Qun, et al. "Practical fixed-time trajectory tracking control of constrained wheeled mobile robots with kinematic disturbances." ISA transactions 129 (2022): 273-286.
[5] Amirkhani, Abdollah, et al. "Controlling wheeled mobile robot considering the effects of uncertainty with neuro-fuzzy cognitive map." ISA transactions 100 (2020): 454-468.
[6] Cao, Guoqiang, et al. "Fuzzy adaptive PID control method for multi-mecanum-wheeled mobile robot." Journal of Mechanical Science and Technology 36.4 (2022): 2019-2029.
[7] Dang, Son Tung, et al. "Adaptive backstepping hierarchical sliding mode control for 3-wheeled mobile robots based on RBF neural networks." Electronics 12.11 (2023): 2345.
[8] Qin, Minghuang, et al. "Fractional-order SMC controller for mobile robot trajectory tracking under actuator fault." Systems Science & Control Engineering 10.1 (2022): 312-324.
[9] Tilahun, Aderajew Ashagrie, et al. "Design of an Adaptive Fuzzy Sliding Mode Control with Neuro-Fuzzy system for control of a differential drive wheeled mobile robot." Cogent Engineering 10.2 (2023): 2276517.
[10] Wei, Juntao, and Bing Zhu. "Model predictive control for trajectory-tracking and formation of wheeled mobile robots." Neural Computing and Applications 34.19 (2022): 16351-16365.
[11] Hassan, Najva, and Abdul Salee m. "Neural network-based adaptive controller for trajectory tracking of wheeled mobile robots." IEEE Access 10 (2022): 13582-13597.
[12] Li, Li, et al. "Trajectory tracking control for a wheel mobile robot on rough and uneven ground." Mechatronics 83 (2022): 102741.
[13] Ebadi, Kamak, et al. "Present and future of slam in extreme environments: The darpa subt challenge." IEEE Transactions on Robotics 40 (2023): 936-959.

[14] Yang, Jung-Min, and Jong-Hwan Kim. "Sliding mode motion control of nonholonomic mobile robots." IEEE Control Systems Magazine 19.2 (1999): 15-23.
[15] Sun, Zhe, et al. "Fuzzy adaptive recursive terminal sliding mode control for an agricultural omnidirectional mobile robot." Computers and Electrical Engineering 105 (2023): 108529.
[16] Xie, Hao, et al. "Robust tracking control of a differential drive wheeled mobile robot using fast nonsingular terminal sliding mode." Computers & Electrical Engineering 96 (2021): 107488.
[17] Zhang, Haichao, et al. "Nonsingular recursive-structure sliding mode control for high-order nonlinear systems and an application in a wheeled mobile robot." ISA transactions 130 (2022): 553-564.
[18] Edwards, Christopher, and Sarah K. Spurgeon. Sliding mode control: theory and applications. Crc Press, 1998.
[19] Gambhire, S. J., et al. "Review of sliding mode based control techniques for control system applications." International Journal of dynamics and control 9.1 (2021): 363-378.
[20] Huang, Yao, Lidong Zhang, and Zhenzhong Chu. "Robust exponential visual regulation of wheeled mobile robots based on active disturbance rejection control." Robotic Intelligence and Automation 45.2 (2025): 187-196.
[21] Moudoud, Brahim, Hicham Aissaoui, and Mohammed Diany. "Extended state observer-based finite-time adaptive sliding mode control for wheeled mobile robot." Journal of Control and Decision 9.4 (2022): 465-476.
[22] Peng, Jiguang, Hanzhen Xiao, and Guanyu Lai. "Nonlinear disturbance observer incorporated model predictive strategy for wheeled mobile robot's trajectory tracking control." International Journal of Control, Automation and Systems 22.7 (2024): 2251-2262.
[23] Miranda-Colorado, Roger. "Observer-based finite-time control for trajectory tracking of wheeled mobile robots with kinematic disturbances." ISA transactions 148 (2024): 64-77.
[24] Hou, Ming, et al. "Hierarchical sliding mode control combined with nonlinear disturbance observer for wheeled inverted pendulum robot trajectory tracking." Applied Sciences 13.7 (2023): 4350.
[25] Zhao, Lv, Jie Jin, and Jianqiang Gong. "Robust zeroing neural network for fixed-time kinematic control of wheeled mobile robot in noise-polluted environment." Mathematics and Computers in Simulation 185 (2021): 289-307.
[26] Nguyen, Thanh Long, Xuan Sinh Mai, and Phuong Nam Dao. "A robust distributed model predictive control strategy for Leader–Follower formation control of multiple perturbed wheeled mobile robotics." European Journal of Control 81 (2025): 101160.
[27] Xie, Hao, et al. "Robust tracking control of a differential drive wheeled mobile robot using fast nonsingular terminal sliding mode." Computers & Electrical Engineering 96 (2021): 107488.
[28] Li, Ping, et al. "Optimized neural network based sliding mode control for quadrotors with disturbances." Math. Biosci. Eng 18 (2021): 1774-1793.
[29] Zhang, Haichao, et al. "Nonsingular recursive-structure sliding mode control for high-order nonlinear systems and an application in a wheeled mobile robot." ISA transactions 130 (2022): 553-564.
[30] Gao, Xiaoshan, Liang Yan, and Chris Gerada. "Modeling and analysis in trajectory tracking control for wheeled mobile robots with wheel skidding and slipping: Disturbance rejection perspective." Actuators. Vol. 10. No. 9. MDPI, 2021.
[31] Zheng, Yunjun, et al. "Adaptive fuzzy sliding mode control of uncertain nonholonomic wheeled mobile robot with external disturbance and actuator saturation." Information Sciences 663 (2024): 120303.
[32] Rabbani, Muhammad Junaid, and Attaullah Y. Memon. "Trajectory tracking and stabilization of nonholonomic wheeled mobile robot using recursive integral backstepping control." Electronics 10.16 (2021): 1992.
[33] Zheng, Yunjun, et al. "Adaptive trajectory tracking control for nonholonomic wheeled mobile robots: A barrier function sliding mode approach." IEEE/CAA journal of automatica sinica 11.4 (2024): 1007-1021.